

# A CMOS Tracking System Approach for Cell Motility Assays

Cristina Martínez-Gómez<sup>1,2</sup>, Alberto Olmo<sup>1,2</sup>, Gloria Huertas<sup>1,3</sup>, Pablo Pérez<sup>1,2</sup>,  
Andres Maldonado-Jacobi<sup>1,3</sup> and Alberto Yúfera<sup>1,2</sup>

<sup>1</sup>Instituto de Microelectrónica de Sevilla, CSIC- Universidad de Sevilla, Av. Americo Vespucio sn, 41092, Sevilla, Spain

<sup>2</sup>Departamento de Tecnología Electrónica, ETSII, Universidad de Sevilla, Av. Reina Mercedes sn, 41010, Sevilla, Spain

<sup>3</sup>Departamento de Electrónica y Electromagnetismo, F. Física, Universidad de Sevilla, Av. Reina Mercedes sn, 41010, Sevilla, Spain

**Keywords:** ECIS, Bioimpedance, Cell Culture, Cell Location, Cell Motility, Brownian Movement, CMOS.

**Abstract:** This work proposes a method for studying and monitoring in real-time a single cell on a 2D electrode matrix, of great interest in cell motility assays and in the characterization of cancer cell metastasis. A CMOS system proposal for cell location based on occupation maps data generated from Electrical Cell-substrate Impedance Spectroscopy (ECIS) has been developed. From this cell model, obtained from experimental assays data, an algorithm based on analysis of the 8 nearest neighbors has been implemented, allowing the evaluation of the cell center of mass. The path followed by a cell, proposing a Brownian route, has been simulated with the proposed algorithm. The presented results show the success of the approach, with accuracy over 95% in the determination of any coordinate (x, y) from the expected center of mass.

## 1 INTRODUCTION

Cell motility plays an important role in many biological processes, such as embryogenesis, wound cicatrization, immune response, and cancer evolution (Ananthkrishnan, 2007). Tumour cell motility is directly related with the processes of cancer propagation, generating metastasis processes, which is one of the main reason of death related with this injury. The assays in-vitro of cell motility represents a useful tool on the research on mechanism regulation of the cancer cells migration, also to test the efficiency of alternative drugs to combat cancer at cellular level.

The most common methods for studying cell motility are optics, based on microscopy, and with fluorescence techniques. However, since these methods are well established and referenced, they require fluorescence markers, which can interfere on correct function of some proteins, modifying the normal cell evolution (Zhu, 2015). In addition, light application at high intensity levels required for exciting fluorescence compounds, can deliver or generate some toxics elements at cells.

ECIS (Giaever and Keese, 1986) technique allows cell culture research based on impedance measurements done based on cell attachment

performance, to obtain cell properties, cell index, etc. (Grimnes, 2008, Yeh, 2015). ECIS techniques represent a non-invasive method for real time monitoring of cells and definition of cell properties: cell adhesion, motility, drug assays test, cell growing, etc. (Sinclair 2012, Mondal, 2013).

Experimentally, ECIS technique requires of an excitation signal, current (or voltage), applied to obtain a voltage (or current) as response. The bio-impedance information due to cell attachment to the electrode is extracted from the signal response (real and imaginary components, or magnitude and phase (Mansor, 2015). The main problems to be solved for extract this information are two. Firstly, bio-impedance changes due to cell culture measurements must be performed with accuracy using adequate techniques and circuits with high performance (Grimnes, 2008) (frequency programmable voltage/current generators, amplifiers, demodulators, etc). Secondly, data obtained for bio-impedance of electrode-cell system should be decoded to rebuild and find the information sought, in general, number of cells in a culture.

The proposed system shown in Figure 1 can be implemented in CMOS technology. It is composed of a 2D matrix of electrodes, which act as “small sensors” of bioimpedance (Yúfera, 2009), integrated

on the same or similar silicon substrate that employed by the CMOS circuits for measuring and acquisition (Huertas, 2015). The circuits allow row/file selection to drive the actual “pixel” under test, and optimal frequency selection to optimize sensor sensitivity and voltage applied to electrodes.

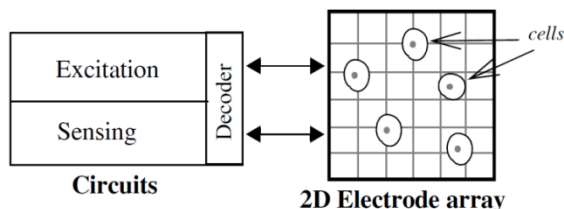


Figure 1: 2D electrode matrix and circuits for excitation and acquisition electrical signals for biompedance test of a cell culture.

The bio-impedance data obtained from cell cultures can be employed to model the 2D system proposed in Figure 1. In particular, it can be defined the fill-factor parameter ( $ff$ ) as the proportional area filled by cell to the total area of one electrode. This parameter oscillated from  $ff=0$ , when the electrode is totally empty of cells (on top), to  $ff=1$ , if the electrode is totally covered of cells. This system gives us a dimensional matrix of numbers, one for each pixel, in the range of 0 to 1, representative of a cell culture status, as illustrated in Figure 2, for a MCF7 cell line image, with an 8x8 electrode array. In this way, black and white images can be created from bio impedance measurements.

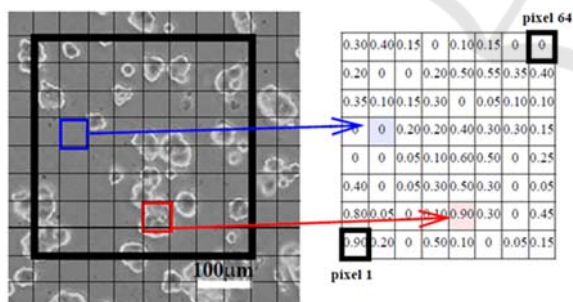


Figure 2: Fill-Factor map associated to each electrode, for a MCF7 cell line image example.

The study proposed in this work focused on spatial-temporal location of a single cell inside an electrode matrix, using for that the information obtained from sensors (pixels), in the form of  $ff$  map. For that, it has been developed a Location Algorithm implemented in Matlab. The proposed algorithm has been applied to solve the problem to define the track followed by a single cell in a culture, determining

the time evolution of its mass centre in a defined period.

This document is organized as follows. Section 2 describes the proposed system structure and the modelling of the cell under study. In section 3 it is detailed how works the algorithm for locating a cell, while section 4 describes its program implementation, the simulations performed and the validation process. Applications for a single cell location and cell tracking will be shown. Finally, section 5 will show the results obtained, and some conclusions of the work, demonstrating the correctness of the proposed algorithm to be applied to study the metastasis problem.

## 2 SYSTEM MODELING

In this section, the proposed system structure to develop the location algorithm is described. The first step is addressed to model the cell which will be used in the case study. There exists a wide variety of cells with very different shapes and structures. For the sake of simplicity, a circular cell is chosen in such a way that it is defined by both the location of the center of the circle ( $x, y$ ) as well as the radio ( $r$ ). It should be taken into account that the circular cell modelling is an ideal model and that elliptic morphologies with variable radio could best conform to the reality.

Once the shape and the size of the cell have been specified, the second step is to define the bidimensional array of electrodes. An array  $M$  of  $N \times N$  dimension, where each element  $M(i, j)$  includes an electrode of fixed area, being  $i$  the position of the row and  $j$  the position of the column. The array  $M$  stores in each element its corresponding  $ff$ , generated by the electrodes. These electrodes of the array are considered squared and the side  $l$ .

To make easier the search algorithm and to avoid, in advance, complex cases to be analysed, when the cell is being located, the size of every element of the array has taken equal or minor to the cell diameter. The dimension of every element or pixel (electrode) of the bidimensional array is equal to the cellular diameter.

A series of concepts required during the development of the system are defined below:

- Center of mass ( $cm$ ): The center of mass of a discrete masses system is a weighted average, according to the individual mass, of the positions of all the particles that compose it. It can be calculated as:

$$\vec{r}_{cm} = \frac{\sum_i m_i \vec{r}_i}{\sum_i m_i} = \frac{1}{M} \sum_i m_i \vec{r}_i \quad (1)$$

$M$ , the total mass of the particle system

$m$ , the mass of the  $i$ -th particle

$\vec{r}_i$ , position vector of the  $i$ -th mass with respect to the assumed reference system.

- Relative error ( $\varepsilon$ ): Is the quotient obtained by dividing the absolute error and the exact value, being the absolute error the difference between the exact value and the measured value.

$$\varepsilon = \frac{|v_{exact} - v_{measured}|}{v_{exact}} \times 100 \quad (2)$$

### 3 LOCATION ALGORITHM

The goal of the proposed algorithm is to obtain the center of mass ( $cm$ ) of the cell, for a given and fixed occupation map, based on the  $ff$  or occupancy levels of the different electrode array elements. With this objective, an iterative algorithm has been developed which assigns weights to each element of array according to whether the 8 adjacent elements contain occupancy values. In the algorithm, several elements are defined:

- **The occupation array  $M$**  above defined, which includes the fill factor values. It represents the data entry and is obtained previously as a result of measurements made on the system.
- An empty **subdivision array  $M_s$**  of  $2N \times 2N$  dimensions, is also defined. It represents the subdivision of the occupation array, where each element  $M(i, j)$  is split into four. This subdivision allows a more precise calculation of which areas of each element are occupied by the cell. In each iteration of the algorithm, the  $M_s$  array is subdivided into 4 sub-elements and so on until an optimal result is reached. The greater the number of divisions, the more accurate the calculated center of mass, but also the longer the required runtime. This array stores the weights that indicate which elements of it are parts of the area of the cell under study (see Figure 3).

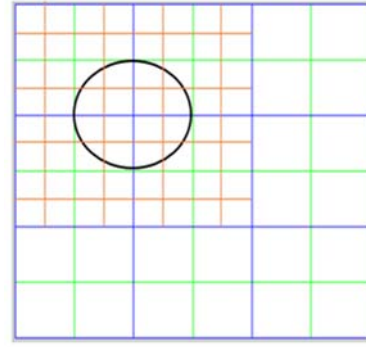


Figure 3: Array  $M$  of  $3 \times 3$  dimension (blue), array  $M_s$  of  $6 \times 6$  dimension (green) and the subdivision of  $M_s$   $12 \times 12$  (red). The occupation map will have non-null values in the two first elements of the two first rows. The subdivision allows to calculate both which elements are part of the cell and which are not and as a consequence obtaining its area more precisely.

- Taking the modeling references, the cell can occupy a maximum of four elements of the array  $M$ , i.e. there will be at most four non-zero fill factors in the array  $M$ . In this way, an **index vector  $I$**  is defined that contains the positions  $(i, j)$  of these four possible values of  $M$ .
- **Array  $P$**  which stores the central points of the greater weight elements of  $M_s$  adjudicated by the algorithm described later.

The algorithm can be divided into three execution steps:

**Step 1: Initialization:** The occupation map elements of  $M$  have input values given by the filling factors resulting from the experiments. Firstly, an initialization process is performed, according to which the occupation map elements  $M$  are subdivided into 4 sub-elements and the weights are assigned, initializing the matrix  $M_s$ . These initial values are selected according to the algorithm proposed.

**Step 2: Iteration:** Secondly, the iterative process is developed where the subdivision array, which contains the weights, is subdivided into 4 sub-elements and so on, at each iteration. At each level of the iteration process, the current area resulting from the algorithm is calculated. The process ends when the areas obtained from the selected sub-elements, for a determined level of iteration, are the closest to the occupancy values obtained by the sensors ( $ff$ ).

**Step 3: Calculation of the Mass Center:** The center of mass is calculated according to the results obtained. From the resulting center of mass, the  $ff_s$  corresponding to this point, called in the algorithm  $ff_{fb}$ , are calculated and compared with the real  $ff_s$  of the given occupation map. With this step, the system is feedback in such a way that the mass center is recalculated according to the difference obtained between the calculated and actual  $ff$ , causing a translation of the center of mass. This recalculation process reduces the error in most of the cases.

The actions involved in each of the algorithm steps are described below in a more detailed way:

**Step 1.- Initialization**

This step begins by traversing the  $M$  array, which initially contains the values of the filling factors resulting from biomedical experimentation. The goal is to assign values to the subdivision array  $M_s$ .

Starting from each element  $M(i,j)$  with a non-zero value and smaller than 0.75, weights are assigned to the four sub-elements of the array  $M_s$ , which correspond to this element  $M(i,j)$ . The assigned weights are determinate by the values of the 8 adjacent elements of  $M(i,j)$ . In particular, the weights will depend on:

- If the neighbor of the diagonal contains a non-zero value, then a constant  $A$  will be added to the element  $M_s$  adjacent to the diagonal (see Figure 4).

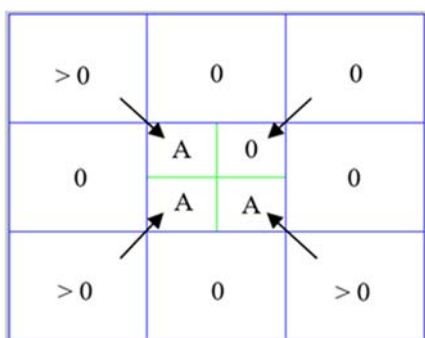


Figure 4: It depicts the diagonal adjacency of the central element. For each adjacent neighbor of the diagonal of  $M$  (blue), a weight  $A$  is assigned to the corresponding element of the array  $M_s$  (green).

- If the remaining neighbors, which do not conform the diagonal, contain a non-zero value, then a constant  $A$  will be added to the

two elements of  $M_s$  adjacent to the sides (see Figure 5).

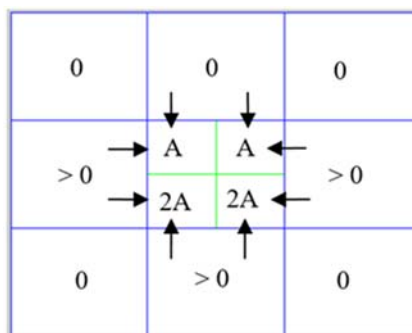


Figure 5: For each 4-adjacent neighbor of the array  $M$  (blue), a constant value  $A$  is assigned to the two corresponding elements of the array  $M_s$  (green).

With this in mind, an element of  $M_s$  will have at most a weight of  $3A$ .

On the other hand, if the value is higher than 0.75, the maximum weight,  $3A$ , is straightaway assigned to the 4 sub-elements ( $M_s(2i-1,2j-1)$ ,  $M_s(2i-1,2j)$ ,  $M_s(2i,2j-1)$ ,  $M_s(2i,2j)$ .

The array  $M$  is again examined and the following conditions are established:

- If  $0 < M(i,j) \leq 0.25$ , only the two larger weight sub-elements of the four possible sub-elements that would form  $M(i,j)$  are stored in the array  $M_s$ .
- If  $0.25 < M(i,j) \leq 0.50$ , the three larger weight sub-elements are stored in.
- If  $M(i,j) > 0.50$ , the four sub-elements of  $M_s$  are stored.

**Step 2.- Iterative process**

In this step the iterative process starts in order to increase the resolution to obtain the area that most closely matches the real area of the cell under study. In each iteration the  $M_s$  array increases its dimension as  $2^{numIter+1}N$ , being  $numIter$ , the iteration number in which the process is and  $N$  the dimension of the  $M$  array.

As in step 1, the  $M_s$  array is examined and weights are assigned to the new subdivision array,  $M_{s\_iter}$ , according to the values of the adjacent elements of  $M_s$ . Calculating the weights of the new array  $M_{s\_iter}$  elements, those that contain the maximum weight with the same criteria established in step 1 are selected. With these elements the approached occupation area is calculated. As in each iteration the subdivision increases, the area that represents each element decreases and thus, the

percentage of occupation area of each element will be given by:

$$4^{-1-numIter} \quad (3)$$

At this point, the proposed by the algorithm occupation area is evaluated, and compared to the initial area, to which it must converge. If the estimated by the algorithm area is equal to the corresponding  $ff$  or approaches to a set range within error margins, the iterative process is terminated. Otherwise, step 2 is repeated to a maximum of 8 iterations. Once the iterative process is completed, the geometric centers of the higher-weight elements of the  $M_{s\_iter}$  array are stored in the array  $P$ . And in turn, the mass center is calculated for each element of index  $I$ , this calculation is based on the points  $P$  contained within such elements. As discussed, there will be a maximum of four  $ff$  values and therefore four mass centers, calculated as follows:

$$\vec{r}_{cm_k} = \frac{1}{M} \sum_{i,j,k} ff_k P(i,j) = \sum_{i,j,k} ff_k P(i,j) \quad (4)$$

where  $k$  defines the  $k$ -th value of the  $I$  vector and  $M$  defines the total mass of the system, in our case, is the sum of the  $ff$  whose value is always unitary.

### Step 3.- Mass center of the cell calculation

The iterative process results in the four mass centers related to each  $ff$ . With these points and following the above equation, it is calculated the mass center of the whole set corresponding to the mass center of the cell.

$$\vec{r}_{cm_{cell}} = \sum_k ff_k \vec{r}_{cm_k} \quad (5)$$

To verify that the result is correct, our system is feedback. The percentage of area occupied by the obtained cell ( $ff_{fb}$ ) is calculated, and it is compared with the original  $ff_s$ . The fill factor and the mass center of the cell are recalculated:

$$\vec{r}_{cm_{cell,fb}} = \sum_k ff_k + (ff_k - ff_{fd_k}) \vec{r}_{cm_k} \quad (6)$$

## 4 SOFTWARE IMPLEMENTATION

The algorithm has been implemented in the mathematical software tool Matlab. We divide this section in two sections where different simulation studies are carried out. First, in sub-section 4.1, an

example of the cellular localization based on the localization algorithm is performed. Secondly, the study and simulation of the cell trajectory described in subsection 4.2 is implemented in Matlab.

### 4.1 Cellular Localization

In this section, an example of the operation and results obtained with an array of 6x6 electrodes and a 10 $\mu$ m diameter cell is shown. To properly simulate the operation of cell cultures, the generation of the position that the cell occupies on the surface of the array is done in a random way. Once the mass center is defined, the occupation map to be used by the algorithm is calculated. Figure 6 shows an example of the map obtained from a cell with center  $cm_{real}$  (13 $\mu$ m, 48 $\mu$ m).

0.02	0.23	0	0	0	0
0.12	0.63	0	0	0	0
0	0	0	0	0	0
0	0	0	0	0	0
0	0	0	0	0	0
0	0	0	0	0	0

Figure 6: Occupation map of a cell with center in the coordinates  $(x,y) = (13\mu\text{m}, 48\mu\text{m})$ .

After five cycles of iteration, a set of points is obtained, from which the center of the cell will be calculated (Figure 7). Specifically two possible centers are obtained, corresponding to the execution of the algorithm without feedback ( $cm_{cell}$  (12.63 $\mu$ m, 47.99 $\mu$ m)) and with feedback ( $cm_{cell,fb}$  (12.87 $\mu$ m, 47.96 $\mu$ m)). The original cell is compared with the two generated results and the relative error is calculated with equation (7).

$$\varepsilon = \frac{|cm_{real} - cm_{cell}|}{cm_{real}} \times 100 \quad (7)$$

For the Y axis case both results are approximated with an error lower than 0.05%. However, for the X axis the error is reduced using feedback (from 2.8% to a 1.0%). In Figure 8 it is shown how calculated cells match real ones.

### 4.2 Cell Trajectory: Brownian Motion

The ECIS technique opens the possibility of monitoring a cell culture in real time. In addition to the estimation of the cellular location from a map of

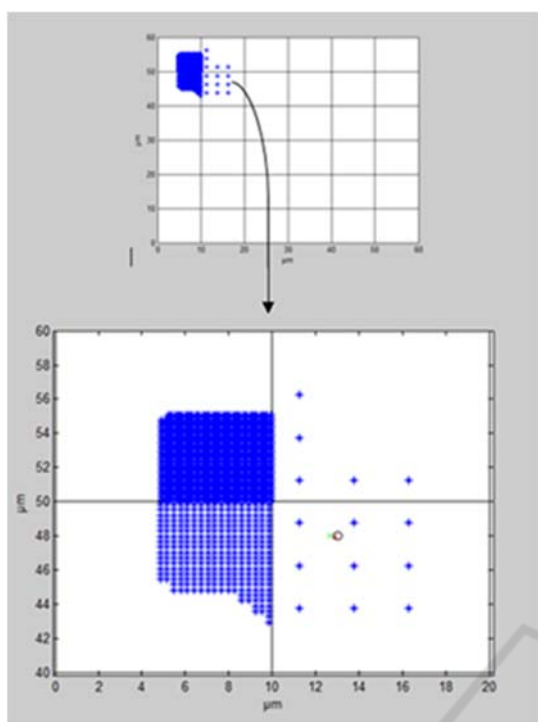


Figure 7: Resulting set of points for the elements with the higher weight, corresponding to the elements of the occupation map. In the selected part it is shown the real centre  $cm_{real} (13\mu m, 48\mu m)$  (blue circle), the center obtained with the algorithm  $cm_{cell} (12.63\mu m, 47.99\mu m)$  (green line) and the center obtained with feedback  $cm_{cell\_fb} (12.87\mu m, 47.96\mu m)$  (red line).

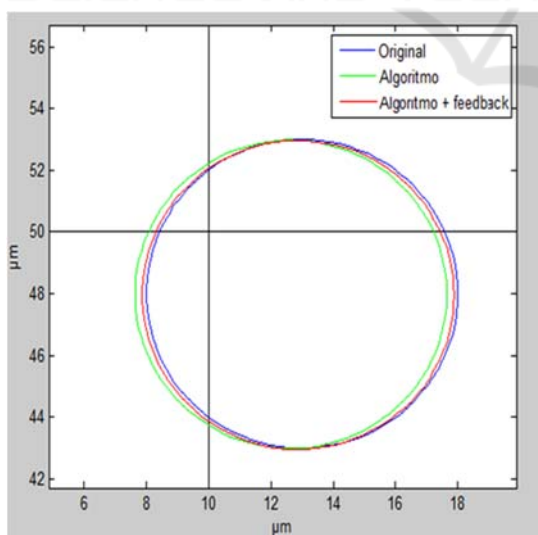


Figure 8: Comparison of the original cell (blue line) with the calculated cell without feedback (green line) and the calculated cell with feedback (red line).

occupation obtained with this technique, it is interesting to have tools to analyze the temporal evolution of the cell. In this way, the trajectories described by them could be analyzed.

The mathematical modeling of cell movement is of great relevance in the fields of biology and medicine. Movement models can take many different forms, but the most commonly used are based on the extensions of simple random motion processes. Assuming that motion is allowed in any direction, this process is essentially known as Brownian motion (Wu 2014, Qu, 2010). The physical phenomenon of Brownian motion is based on the random motion of particles suspended in a fluid as a result of their collision with rapidly moving atoms or molecules.

To generate a two dimensional random motion, two independent random paths are used, one for each coordinate in time using different random seeds. Instead of using random steps from a Gaussian distribution, an approximation to Brownian motion can be constructed by taking random measurements of simple probability functions, such as a delta function or a constant probability density function (Codling 2018).

A Brownian motion model is implemented in Matlab, indicating the starting point from which the cell will start and the number of time samples desired to obtain the points of the trajectory. Random angles are generated for each moment and each mass center is produced following a stochastic process:

$$\begin{aligned} cm_x(t) &= cm_x(t - 1) + \cos \sigma(t) \\ cm_y(t) &= cm_y(t - 1) + \sin \sigma(t) \end{aligned} \quad (8)$$

In addition, the generation of the trajectory is limited according to the size of the culture matrix.

Figure 9 and 10 show a possible trajectory generated by the cell under study. After obtaining the occupation map for each time instant, it is simulated the trajectory followed using the localization algorithm, previously implemented. To be specific, it is considered a cell with an average velocity of  $0.1 \mu m/min$ . The example simulates the calculation of sixteen occupation maps for three hours.

As we checked in the previous point, most of the points obtained with feedback are closer to the real points. Table 1 shows for each point the errors committed without feedback and with feedback, the number of iterations made and the time used by the system. The measurements have been obtained using an Intel® Core™ i7-4501U processor at 2.60GHz and 11.9GB of RAM.

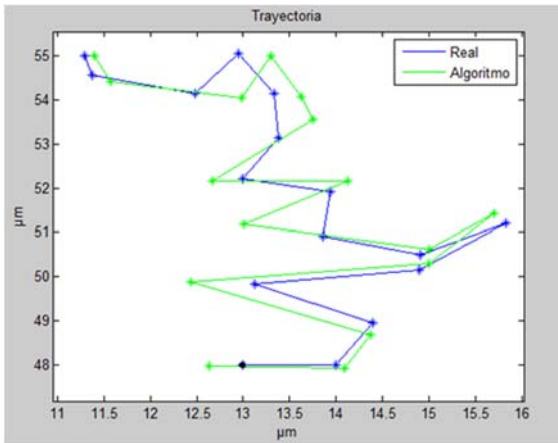


Figure 9: Real trajectory of a cell with radius  $10\mu\text{m}$  (blue) and trajectory calculated with the localization algorithm (green).

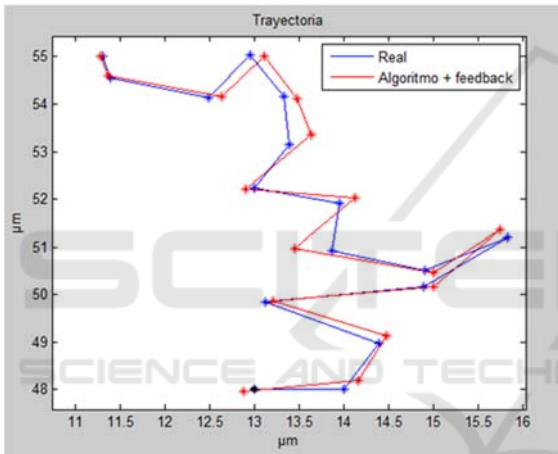


Figure 10: Real trajectory of a cell with radius  $10\mu\text{m}$  (blue) and trajectory calculated with the localization algorithm with feedback (red).

With these results we can verify that in most cases the error decreases applying the feedback process, being position 2 and 3 the only points where the error is not improved. Even in these cases, errors less than 3% are obtained. The majority of iterations required to obtain the position is two cycles, reducing the overall execution time of the trajectory. For iterations less than 8 cycles the time spent is less than 60 seconds.

To confirm that the system developed in this work is capable of robustly and accurately estimating the position of the cell from the occupation maps, an empirical study with more samples has been carried out. These tests consist of the random generation a cell track, with fifty points, each one with their corresponding maps of occupation. The position estimation of each of the cells generated applying the

Table 1: Error percentage for the 16 positions.

Pos	Relative error ( $\epsilon$ )		N_ite	CPU(s)
	Axis x	Axis y		
1	Alg	2.85%	5	56.70
	Alg + fb	1.00%		
2	Alg	0.67%	5	55.02
	Alg + fb	1.12%		
3	Alg	0.12%	8	70.50
	Alg + fb	0.53%		
4	Alg	5.21%	4	54.6
	Alg + fb	0.64%		
5	Alg	0.74%	2	54.01
	Alg + fb	0.74%		
6	Alg	0.81%	2	47.69
	Alg + fb	0.49%		
7	Alg	0.67%	2	47.90
	Alg + fb	0.67%		
8	Alg	6.15%	5	49.03
	Alg + fb	2.95%		
9	Alg	1.34%	2	48.21
	Alg + fb	1.30%		
10	Alg	2.51%	5	57.25
	Alg + fb	0.70%		
11	Alg	2.76%	2	48.14
	Alg + fb	1.90%		
12	Alg	2.19%	2	48.01
	Alg + fb	1.07%		
13	Alg	2.68%	4	51.4
	Alg + fb	1.15%		
14	Alg	4.04%	2	49.27
	Alg + fb	1.18%		
15	Alg	1.72%	2	47.90
	Alg + fb	0.16%		
16	Alg	0.90%	2	47.68
	Alg + fb	0.24%		

algorithm and finally, the definition of the position of each point generated applying the algorithm and its feedback.

The highest errors obtained were located when the occupation map collects most of the area in a single element, but with connected elements with a very low value. In contrast, when the cell is more evenly divided into several elements, the error is very small. And in the event that the cell is entirely in one element or divided exactly in two or four elements, the error obtained is null. Table 2 shows the maximum and minimum error percentages obtained, and an estimation of the mean error value.

Table 2: Experimental error percentages.

Relative error ( $\epsilon$ )		Max.	Min.	Mean
Algorithm	Eje x	8.35%	0%	2.19%
	Eje y	2.69%	0 %	0.49%
Algorithm + Feedback	Eje x	4.98%	0 %	0.95%
	Eje y	1.05%	0 %	0.19 %

With this experimental study, it is concluded that the maximum error that the system can have is below 5% for the X axis and below 1% for the Y axis.

## 5 CONCLUSIONS AND FUTURE WORK

A cellular localization system has been developed based on the occupation maps generated by electrical impedance spectroscopy. The localization system has been able to generate the approximated cell position in a culture, with a maximum relative error of 4.98%, and a typical error of 1%, when it is provided feedback to the algorithm. Although sometimes the feedback does not reduce the error, in most cases improves it, decreasing the error by half. The proposed tracking algorithm enables CMOS technologies for Lab-on-a-Chip systems for cell motility assays, particularly useful in cancer research.

In order to expand the study, possible cellular trajectories have been randomly generated following the modeling of the Brownian system. Starting from the trajectory it will be possible to perform studies on the cellular behavior in different situations of interest, as can be the effects of drugs in the cellular activity.

From the results obtained in this study, new lines of research are opened that can be of great scientific interest. Firstly, the cellular morphology is very uneven and irregular, so the modeling of the cell in a circular form does not resemble the reality, and supposes an excessively simple model. A possible improvement of the system would be to use modeling of cells with more common form, for example, as an ellipse. Tests with real cases can also be carried out, using electrode arrays and a cell line of interest, to characterize its trajectory and study its behavior. Furthermore, variable side electrodes that do not occupy the entire pixel could be used, and study, this way, how to solve dead zones where no information is collected and can be occupied by the cells.

## ACKNOWLEDGEMENTS

This work was supported in part by the Spanish founded Project: TEC2013-46242-C3-1-P: Integrated

Microsystem for Cell Culture Assays, co-financed with FEDER.

## REFERENCES

- Ananthakrishnan, R., Ehrlicher, A., 2007. The Forces Behind Cell Movement. *Int J Biol Sci*, vol. 3, n<sup>o</sup>. 5, pp. 303–317.
- Zhu, Z., Frey O., et al., 2015. Time-lapse electrical impedance spectroscopy for monitoring the cell cycle of single immobilized *S. pombe* cells. *Scientific Reports*, vol. 5, p. 17180.
- Giaever, I. and Keese, C. R., 1991. Micromotion of mammalian cells measured electrically, Proc. Natl. Acad. Sci. USA. *Cell Biology*, vol. 88, pp: 7896-7900.
- Grimnes, S., Martinsen, O., 2008. *Bio-impedance and Bioelectricity Basics*, Academic Press, Elsevier, 2<sup>nd</sup> edition.
- Yeh, C. F. et al., 2015. Towards an Endpoint Cell Motility Assay by a Microfluidic Platform. *IEEE Transactions on NanoBioscience*, vol. 14, n<sup>o</sup>. 8, pp. 835–840.
- Sinclair, A. J. et. al, 2012. Bioimpedance analysis for the characterization of breast cancer cells in suspension. *IEEE Trans Biomed Eng*, vol. 59, n<sup>o</sup>. 8, pp. 2321–2329.
- Mondal, D., RoyChaudhuri, C., 2013. Extended electrical model for impedance characterization of cultured HeLa cells in non-confluent state using ECIS electrodes. *IEEE Trans Nanobioscience*, vol. 12, n<sup>o</sup>. 3, pp. 239–246.
- Mansor, A. F. M., et al., 2015. Cytotoxicity studies of lung cancer cells using impedance biosensor. In *2015 International Conference on Smart Sensors and Application (ICSSA)*, pp. 1–6.
- Huertas, G., Maldonado, A., Yúfera A., et al., 2015. The Bio-Oscillator: A Circuit for Cell-Culture Assays. *IEEE Transactions on Circuits and Systems II*, vol. 62, n<sup>o</sup>. 2, pp. 164–168.
- Yúfera, A., Rueda, A., 2009. A CMOS bio-impedance measurement system. In *12<sup>th</sup> International Symposium on Design and Diagnostics of Electronic Circuits Systems*, pp. 252–257.
- Yúfera, A., Rueda, A., 2010. Design of a CMOS closed-loop system with applications to bioimpedance measurements. *Microelectronics J.* vol. 41, pp.231-239.
- Wu, P. H., et al, 2014. Three-dimensional cell migration does not follow a random walk. *Proc Natl Acad Sci U S A*, vol. 111, n<sup>o</sup>. 11, pp. 3949–3954.
- Codling E. A. et al., 2008. Random walk models in biology. *J R Soc Interface*, vol. 5, n<sup>o</sup>. 25, pp. 813–834.
- Qu B., Addison P. S., 2010. Modelling Flow Trajectories Using Fractional Brownian Motion. In *2010 International Workshop on Chaos-Fractals Theories and Applications (IWCFTA)*, pp. 420–424.